JOURNAL OF PHYSICAL ORGANIC CHEMISTRY
J. Phys. Org. Chem. 2005; **18:** 69–82
Published online 6 July 2004 in Wiley InterScience (www.interscience.wiley.com). DOI: 10.1002/poc.802

Electron transfer reactivity of methyl-substituted amine $NH_n(CH_3)_{3-n}/NH_n(CH_3)_{3-n}^+$ ($n = 0$–3) self-exchange systems: a theoretical investigation

Qiao Sun,[1,2] Yuxiang Bu,[1,2]* Lixiang Sun,[1] Shihai Yan[1] and Xueli Cheng[2]

[1]Key Laboratory of Colloid and Interface Chemistry of the Ministry of Education, Institute of Theoretical Chemistry, Shandong University, Jinan 250100, China
[2]Department of Chemistry, Qufu Normal University, Qufu 273165, China

Received 4 January 2003; revised 3 June 2003; accepted 4 March 2004

ABSTRACT: The geometries of $NH_n(CH_3)_{3-n}$, $NH_n(CH_3)_{3-n}^+$ ($n = 0$–3) and their corresponding coupling complexes $[NH_n(CH_3)_{3-n}\cdots NH_n(CH_3)_{3-n}^+$ ($n = 0$–3)] were determined using density functional theory (DFT) and *ab initio* methods at the 6–311+G* basis set level, and the relative stability is predicted to decrease in the order $H_3N\cdots NH_3^+ > CH_3H_2N\cdots NH_2CH_3^+ > (CH_3)_2HN\cdots NH(CH_3)_2^+ > (CH_3)_3N\cdots N(CH_3)_3^+$ for the four stable encounter complexes. The inapplicability is also discussed for the DFT methods in predicting the dissociation energy curves especially with long contact distance in which the DFT methods give abnormal behavior for the dissociation of the complexes due to the 'inverse symmetry breaking' problem. The contact distance dependences of the activation energy, the coupling matrix element and the electron-transfer (ET) rate were determined with the MP2/6–311+G* or MP2/6–31G* method. The results show that ET reactions occur chiefly only over a small range of contact distances where the favorable ones are $1.9\,\text{Å} < R_{N\cdots N} < 4.0\,\text{Å}$ for $NH_3\cdots NH_3^+$, $2.5\,\text{Å} < R_{N\cdots N} < 5.0\,\text{Å}$ for $CH_3H_2N\cdots NH_2CH_3^+$, $2.1\,\text{Å} < R_{N\cdots N} < 5.0\,\text{Å}$ for $(CH_3)_2HN\cdots NH(CH_3)_2^+$ and $3.2\,\text{Å} < R_{N\cdots N} < 6.0\,\text{Å}$ for $(CH_3)_3N\cdots N(CH_3)_3^+$ coupling systems. The most optimum contact distances for the above four coupling systems are 2.4, 3.0, 2.7 and 3.7 Å where the corresponding maximum ET rates are $2.53\times10^5\,s^{-1}(H_3N\cdots NH_3^+)$, $1.16\times10^3\,s^{-1}(CH_3H_2N\cdots NH_2CH_3^+)$, $7.55\times10^{-3}\,s^{-1}$ $[(CH_3)_2HN\cdots NH(CH_3)_2^+]$ and $2.25\times10^{-4}\,s^{-1}$ $[(CH_3)_3N\cdots N(CH_3)_3^+]$, respectively, and the corresponding maximum ET rate order is $H_3N\cdots NH_3^+ > CH_3H_2N\cdots NH_2CH_3^+ > (CH_3)_2HN\cdots NH(CH_3)_2^+ > (CH_3)_3N\cdots N(CH_3)_3^+$. Increasing substituents on the active N centers may significantly change the ET rate and other kinetic parameters. Copyright © 2004 John Wiley & Sons, Ltd.

KEYWORDS: electron transfer reactivity; DFT method; activation energy; coupling matrix element; *ab initio* calculation; substituted amine couples

INTRODUCTION

Ammonia and the saturated aliphatic amines have been investigated extensively[1–5] owing to their wide applications, such as in making pesticides, medicines, coloring matters and ion-exchange colophony and their wide existence in nature and biological organisms. In biological systems, they are linked to amino acid residues and other biological molecular chains, and the interactions among them and other biological active ions play an important role in assisting biological functionality. In particular, there are two important processes in biological systems, photosynthesis and respiration processes. In both processes, electron transfer (ET) and proton translocation make up their main contents. Obviously, the intermediate molecular fragments linked to the donor/acceptor active sites play the dominant role in assisting and promoting the ET and the proton translocation and thus affect the biological functionality. Therefore, it is fundamental to explore the coupling interaction modes and the ET reactivity of these systems for further understanding of the biological functional mechanism. However, systematic studies of the different structural properties regarding ammonia and some methyl-substituted aliphatic amines and the complexes formed between the neutral molecule [NH_3, NH_2CH_3, $NH(CH_3)_2$ or $N(CH_3)_3$] and their cations [NH_3^+, $NH_2CH_3^+$, $NH(CH_3)_2^+$ or $(CH_3)_3^+$] have not been reported elsewhere. In this paper, we focus on the complexes formed between the neutral monomers [NH_3, NH_2CH_3, $NH(CH_3)_2$ and $N(CH_3)_3$] and the their corresponding cation monomers [NH_3^+, $NH_2CH_3^+$, $NH(CH_3)_2^+$ and $N(CH_3)_3^+$] (Fig. 1) and their ET reactivity.

**Correspondence to:* Y.-X. Bu, Key Laboratory of Colloid and Interface Chemistry of the Ministry of Education, Institute of Theoretical Chemistry, Shandong University, Jinan 250100, China.
E-mail: byx@sdu.edu.cn
Contract/grant sponsor: National Natural Science Foundation of China; *Contract/grant number:* 20273040.
Contract/grant sponsor: Natural Science Foundation of Shandong Province; *Contract/grant sponsor:* SRFDP.

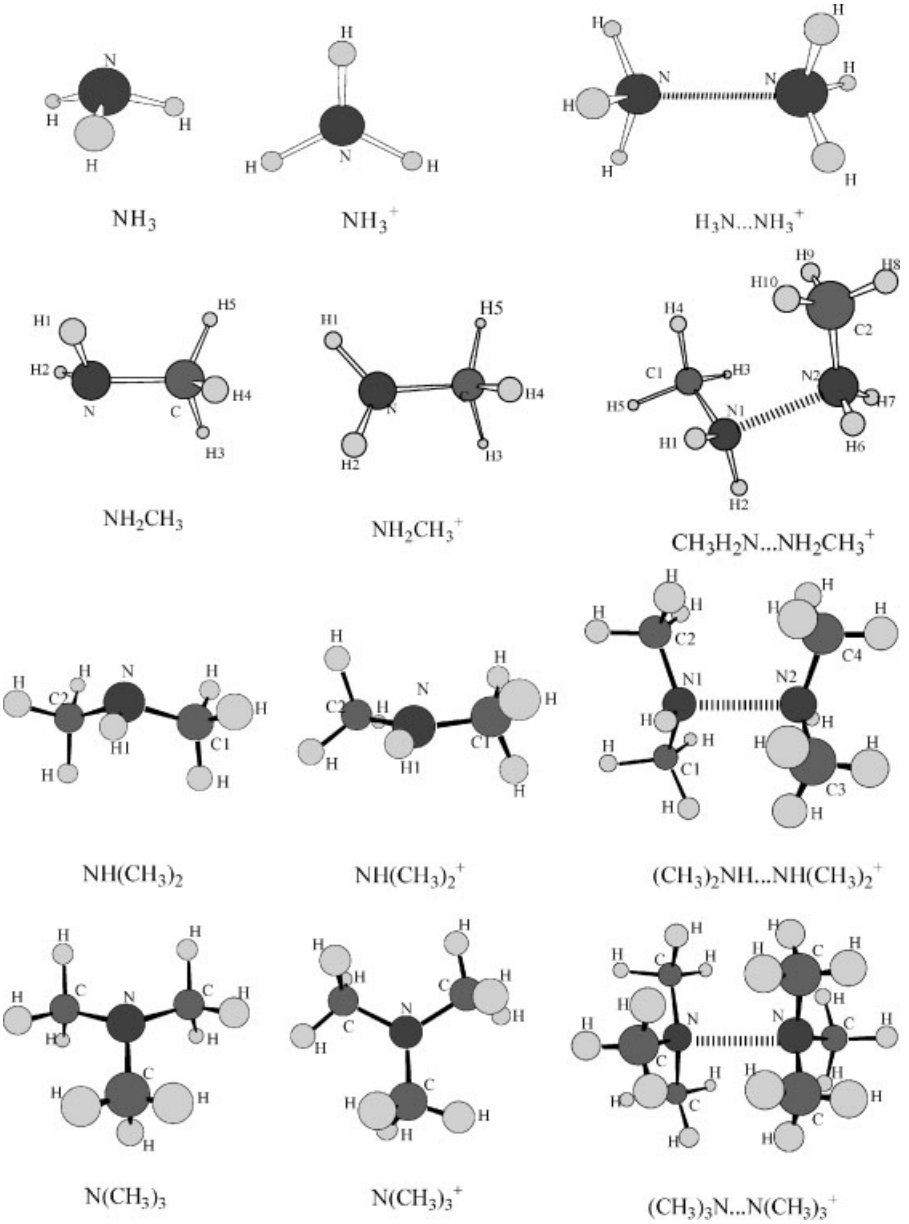

Figure 1. Atomic numbering corresponding to the geometric parameters of the four neutral single molecules [NH_3, NH_2CH_3, $NH(CH_3)_2$ and $N(CH_3)_3$], the four single molecule cations [NH_3^+, $NH_2CH_3^+$, $NH(CH_3)_2^+$ and $N(CH_3)_3^+$], single molecules and the four complexes [$H_3N\cdots NH_3^+$, $CH_3H_2N\cdots NH_2CH_3^+$, $(CH_3)_2HN\cdots NH(CH_3)_2^+$ and $(CH_3)_3N\cdots N(CH_3)_3^+$]

In the last two decades, ET reactions have continued to be the subject of many theoretical[6–8] and experimental[9–11] studies, for both chemical and biological systems. In general, ET can occur in a determinate range of contact distances, although there is a maximum reaction probability for each ET system at an optimum contact distance. However, for a real system, especially for the biological systems, since the active donor/acceptor groups are generally fixed to the biological molecular chains, the structural constraint and the solvent fluctuation perhaps cannot assuredly give the donor/acceptor species an optimum interaction mode for favoring ET like that for a gas-phase isolated coupling couple. Also, the coupling mode for ET or proton transfer may vary as the surroundings change. Therefore, it is very interesting to investigate the ET reactivity of a system at different contact distances and the effect of the coupling mode on the ET mechanism. Although there are many publications aimed at the ET reactivity of various systems, there is a serious lack of studies on the coupling mode (including contact distance and orientation, etc.) dependence of the ET reactivity for any systems. In detail, for the ammonium ion pair, studies on the interaction modes and the ET mechanism have not yet been reported. Therefore, in this paper, taking the $NH_n(CH_3)_{3-n}/NH_n(CH_3)_{3-n}^+$ pair as model species, accurate descriptions of the kinetics parameters of self-exchange ET reactions of $NH_n(CH_3)_{3-n}$ and $NH_n(CH_3)_{3-n}^+$ will be made, and

the contact distance dependence of various kinetic parameters such as activation energy, coupling matrix element and the ET rate of the $NH_n(CH_3)_{3-n}\cdots NH_n(CH_3)^+_{3-n}$ coupling system will be analyzed.

In addition, in view of the complicated nature of the biological macromolecule and the computational cost at wavefunction-correlated *ab initio* theoretical levels, computational methods based on density functional theory (DFT) are widely used. These methods can predict relatively accurate molecular structures and vibrational frequencies with moderate computational effort for equilibrium systems. However, for the above ET systems, the occurrence of ET must not require the donor and acceptor to be in the most favorable geometry and interaction mode. Once the ET condition is met, transfer may occur with considerable probability no matter whether the coupling system is in equilibrium or non-equilibrium geometry. In order to explore the ET reactivity of the system at a far from equilibrium geometry, we must determine the potential surface of the system at that far from equilibrium geometry. Therefore, this work also presents a challenge for theoretical calculational methods as to whether or not they are suitable for calculations on systems at a geometry far from equilibrium.

A recent study has indicated that the energy curves with some DFT methods (such as B3LYP and B3P86) show an abnormal dissociation behavior. This abnormal behavior was first reported by Bally and Sastry in 1997[12] and was recognized to be attributable to the 'inverse symmetry breaking' problem. In view of this consideration, another aim of this study was to check the applicability of DFT methods and wavefunction-correlated *ab initio* methods in predicting the energy curves especially with long contact distance, and to test the abnormal behavior. Therefore, for the sake of comparison, both DFT and Møller–Plesset theory methods are used in this paper.

THEORETICAL MODEL

The self-exchange ET reaction between the neutral $NH_n(CH_3)_{3-n}$ and its cation can be expressed as

$$NH_n(CH_3)_{3-n}(R_1) + NH_n(CH_3)^+_{3-n}(R_2) = NH_n(CH_3)^+_{3-n}(R_2) + NH_n(CH_3)_{3-n}(R_1) \quad (1)$$

where R_1 and R_2 denote the characteristic parameters such as bond lengths, bond angles and dihedral angles of the neutral $NH_n(CH_3)_{3-n}$ and its cation, respectively.

The ET reaction between the donor $[NH_n(CH_3)_{3-n}]$ and the acceptor $[NH_n(CH_3)^+_{3-n}]$ may be expressed by five elementary processes:

1. Formation of the encounter complex:

$$NH_n(CH_3)_{3-n}(R_1) + NH_n(CH_3)^+_{3-n}(R_2) \rightleftharpoons NH_n(CH_3)_{3-n}(R'_1)\cdots NH_n(CH_3)^+_{3-n}(R'_2) \quad (2)$$

2. Reorganization of the encounter complex:

$$NH_n(CH_3)_{3-n}(R'_1)\cdots NH_n(CH_3)^+_{3-n}(R'_2) \rightarrow NH_n(CH_3)_{3-n}(R^*_1)\cdots NH_n(CH_3)^+_{3-n}(R^*_2) \quad (3)$$

3. Electron transfer:

$$NH_n(CH_3)_{3-n}(R^*_1)\cdots NH_n(CH_3)^+_{3-n}(R^*_2) \rightarrow NH_n(CH_3)^+_{3-n}(R^*_1)\cdots NH_n(CH_3)_{3-n}(R^*_2) \quad (4)$$

4. Relaxation of successor activated complex:

$$NH_n(CH_3)^+_{3-n}(R^*_1)\cdots NH_n(CH_3)_{3-n}(R^*_2) \rightarrow NH_n(CH_3)^+_{3-n}(R''_2)\cdots NH_n(CH_3)_{3-n}(R''_1) \quad (5)$$

5. Dissociation of successor complex:

$$NH_n(CH_3)^+_{3-n}(R''_2)\cdots NH_n(CH_3)_{3-n}(R''_1) \rightarrow NH_n(CH_3)^+_{3-n}(R_2) + NH_n(CH_3)_{3-n}(R_1) \quad (6)$$

Obviously, the product of Eqn (2) is the encounter complex, and may have various different structures. Equation (2) is the pre-equilibrium equation; the energy change corresponds to the sum of the electrostatic work required to bring the reactants together with the contact distance, $R_{N—N}$, and the stabilization energy. The energy change in Eqn (3) corresponds to the activation energy, and the corresponding R'_1, R'_2, R^*_1 and R^*_2 are the geometric parameters at the encounter complex state (the initial state) and the activated state at a definite contact distance, $R_{N—N}$, respectively. Obviously, they are the functions of $R_{N—N}$. Actually, when two species, $NH_n(CH_3)_{3-n}(R_1)$ and $NH_n(CH_3)^+_{3-n}(R_2)$, encounter via molecular diffusion at an arbitrary contact distance, if the ET condition is met, the ET may occur no matter they are at the stable encounter state or not. Therefore, the encounter complexes with R'_1 and R'_2 geometries are essentially assumed states and they are not surely stable states except for that at the most optimum contact distance (the fully optimized geometry).

Many quantum mechanical theories have been successfully used to discuss the relationship between the ET rate and some parameters.[13,14] Among these theories, the Golden rule is an excellent one, which has been successfully applied to dealing with ET of $O_2 + O_2^-$ and hydrogen-transfer tunneling reactions.[15,16] In this paper, the Golden rule is also used to discuss the ET reactivity of the $NH_n(CH_3)_{3-n}\cdots NH_n(CH_3)^+_{3-n}$ coupling system. According to the Golden rule, the ET rate can be expressed as the following equation:

$$k_{et}(R_{N-N}) = (4\pi^2/h)|H_{if}(R_{N-N})|^2 FC(R_{N-N}) \quad (7)$$

where H_{if} is the matrix element coupling between the two redox sites, FC is the Franck–Condon factor and h is Planck's constant.

A simple formalism of the coupling matrix element can be expressed by the following equation, which has been successfully used to calculate ET kinetic parameters of many systems:[14,17]

$$H_{if}(R_{N-N}) = E_d - E_a(R_{N-N}) \tag{8}$$

where H_{if} actually represents the energy difference between the non-adiabatic activated state and the adiabatic activated state. $E_a(R_{N—N})$ denotes the adiabatic activation energy at the contact distance, $R_{N—N}$, and E_d denotes the non-adiabatic activation energy, which is the energy of the reacting system at the crossing point under assumption that the reacting system experiences a non-adiabatic electron transmission process.

FC originates from the requirement (Franck–Condon principle) that the nuclear configuration of the reactants must meet the energy conservation condition that the energy of the reactants and products are equal at the transition state (this occurs via thermal fluctuations and/or vibrations).

There are two that factors influence *FC* factor, the free energy and the reorganization energy. The *FC* factor may be directly expressed as a simple formalism:

$$FC(R_{N-N}) = [4\pi E_\lambda(R_{N-N})RT]^{-1/2}\exp[-E_a(R_{N-N})/RT] \tag{9}$$

where $E_\lambda(R_{N—N})$ and $E_a(R_{N—N})$ denote reorganization energy and activation energy at different contact distances, respectively, and T is the thermodynamic temperature. Approximately, for a thermoneutral exchange process, $E_\lambda = 4E_a$.

At the activated state, the energy of the activated complex $NH_n(CH_3)_{3-n}(R_1^*)\cdots NH_n(CH_3)_{3-n}^+(R_2^*)$ before ET can be expressed as the following equation:

$$E_i = E_{NH_n(CH_3)_{3-n}}(R_1^*) + E_{NH_n(CH_3)_{3-n}^+}(R_2^*) \tag{10}$$

After ET, the energy of product may be expressed as

$$E_f = E_{NH_n(CH_3)_{3-n}^+}(R_1^*) + E_{NH_n(CH_3)_{3-n}}(R_2^*) \tag{11}$$

where E_j(R*) denotes the energy of jth molecular fragment species in the reacting complex at the activated state $[NH_n(CH_3)_{3-n}\cdots NH_n(CH_3)_{3-n}^+]$. During the transition, the energy conservation principle requires that $E_f = E_i$. Hence

$$E_{NH_n(CH_3)_{3-n}}(R_1^*) + E_{NH_n(CH_3)_{3-n}^+}(R_2^*) = E_{NH_n(CH_3)_{3-n}^+}(R_1^*) + E_{NH_n(CH_3)_{3-n}}(R_2^*) \tag{12}$$

Since $NH_n(CH_3)_{3-n}$ and $NH_n(CH_3)_{3-n}^+$ are two systems with different properties, Eqn (12) suggests that R_1^* should be equal to R_2^*. Therefore, the energy of the system at activated state can be expressed as

$$E_a^* = E_{NH_n(CH_3)_{3-n}}(R_1^*) + E_{NH_n(CH_3)_{3-n}^+}(R_1^*) \tag{13}$$

Obviously, Eqn (13) represents the activated state energy curve formed in the crossing between the two non-adiabatic potential energy surfaces corresponding to the initial and the final states of the ET, respectively. The corresponding minimum activation energy may be obtained using the minimization method.

The adiabatic activation energy $E_a(R_{N—N})$ can be easily obtained by subtracting the energy of each encounter complex from the corresponding energy at the activated state:

$$E_a(R_{N-N}) = E_{NH_n(CH_3)_{3-n}^+\cdots NH_n(CH_3)_{3-n}}(R_1^*, R_{N-N}) - E_{NH_n(CH_3)_{3-n}^+\cdots NH_n(CH_3)_{3-n}}(R_1, R_2) \tag{14}$$

Actually this state intuitively represents the geometry that the ET is likely to take place.

Analogously, the non-adiabatic activation energy can be obtained by subtracting the energies of $NH_n(CH_3)_{3-n}$ and $NH_n(CH_3)_{3-n}^+$ at their own equilibrium geometries from the total energies of $NH_n(CH_3)_{3-n}$ and $NH_n(CH_3)_{3-n}^+$ at the crossing state:

$$E_d = E_{NH_n(CH_3)_{3-n}}(R_1^*) + E_{NH_n(CH_3)_{3-n}^+}(R_1^*) - E_{NH_n(CH_3)_{3-n}}(R_1) - E_{NH_n(CH_3)_{3-n}^+}(R_2) \tag{15}$$

Namely, E_d is the value of $E_a(R_{N—N})$ at infinite separation, $R_{N—N} = \infty$. Hence the electronic coupling matrix element or the energy reduction caused by the coupling between the initial and the final states of ET may be obtained by

$$H_{if}(R_{N-N}) = E_d - E_a(R_{N-N})$$

$$H_{if}(R_{N-N}) = E_{NH_n(CH_3)_{3-n}}(R_1^*)E_{NH_n(CH_3)_{3-n}^+}(R_1^*) - E_{NH_n(CH_3)_{3-n}^+\cdots NH_n(CH_3)_{3-n}}(R_1^*, R_{N-N}) - E_s \tag{16}$$

$$E_s = E_{NH_n(CH_3)_{3-n}}(R_1) + E_{NH_n(CH_3)_{3-n}^+}(R_2) - E_{NH_n(CH_3)_{3-n}^+\cdots NH_n(CH_3)_{3-n}}(R_1, R_2) \tag{17}$$

where R_1^* is the activated parameter of the reacting complex at the given $R_{N—N}$ contact distance.

CALCULATION DETAILS

DFT (B3P86, B3LYP, B3PW91) and *ab initio* calculation (MP2) at the 6–311+G* basis set level were used to optimize the molecular structures of NH_3, NH_3^+, NH_2CH_3, $NH_2CH_3^+$, $NH(CH_3)_2$, $NH(CH_3)_2^+$, $N(CH_3)_3$, $N(CH_3)_3^+$ and the four complexes formed between

molecules and their cations, $H_3N\cdots NH_3^+$, $CH_3H_2N\cdots NH_2CH_3^+$, $(CH_3)_2HN\cdots NH(CH_3)_2^+$ and $(CH_3)_3N\cdots N(CH_3)_3^+$ (Fig. 1). The stabilization energies of four complexes were also calculated with three DFT methods (B3LYP, B3P86 and B3PW91) and the MP2 method using 6–311+G* or 6–31G* basis sets. The applicability of DFT methods (B3P86, B3LYP, B3PW91) is discussed in exploring the potential energy surfaces at the activated state. Then the MP2 method with the 6–311+G* or 6–31G* basis set was used to scan the potential energy surfaces in order to obtain the relevant energy quantities (such as activation energy), the coupling matrix elements and Franck–Condon factors of these coupling systems. Finally, the contact distance dependence of the kinetic parameters is discussed.

In actual calculations regarding the contact dependence of various kinetic parameters, the contact distance ranges from 2.0 to 10.0 Å. For a given contact distance, the encounter complex is first optimized, then the activated state energy curves are obtained by scanning the geometric parameters (R_1', R_2') from those of the reduced species to those of the oxidized species. In general, during the ET process, all C—H are basically unchanged, therefore, they are set to be the averaged one and kept fixed. Only the N—C, N—H and relevant angles related to the N center vary in scanning the ET PES for a given contact distance. The minimization of the PES may yield the activated parameters (R_1^*/R_2^*, where $R_1^* = R_2^*$ at the activated states). On the basis of Eqn (14)–(17), the relevant kinetic parameters at a certain contact distance can be obtained according to the optimized coupling modes like those in the stable encounter complexes.

All the calculations are performed with the Gaussian 94 program[18] using three density functional methods (B3LYP, B3P86 and B3PW91) and the MP2 method at the 6–311+G* or 6–31G* basis set level. These three DFT models combine the Becke three-parameter hybrid functional, which is a linear combination of Hartree–Fock exchange, the correlation functional of Lee, Yang and Parr,[19,20] Perdew (P86)[21,22] Perdew and Wang (PW91),[23] respectively.

RESULTS AND DISCUSSION

Geometric structures of the neutral monomers [NH_3, NH_2CH_3, $NH(CH_3)_2$, $N(CH_3)_3$] and their cation monomers [NH_3^+, $NH_2CH_3^+$, $NH(CH_3)_2^+$ and $N(CH_3)_3^+$]

The bond lengths (Å) and bond angles (degrees) of NH_3, NH_2CH_3, $NH(CH_3)_2$, $N(CH_3)_3$, NH_3^+, $NH_2CH_3^+$, $NH(CH_3)_2^+$ and $N(CH_3)_3^+$ calculated by the B3P86, B3LYP, B3PW91 and MP2 methods at the 6–311+G* basis set level are summarized in Table 1. From the results, it can be seen that the N—H bond lengths in NH_3 with B3P86 method is 1.0127 Å, and the ∠HNH bond angle is 107.9°, which are in good agreement with the experimental values[24] (1.012 Å for the N—H bond lengths in NH_3 and 106.7° for the ∠HNH bond angle). This indicates that the B3P86 method is more suitable in predicting relatively accurate molecular structures with moderate computational effort. For NH_3^+ species, the N—H bond lengths and the ∠HNH bond angle obtained by the MP2 method are 1.0195 Å and 120.0°, respectively, which is also in good agreement with the experimental results[25] (the N—H bond length is 1.020 Å and the ∠HNH bond angle is 120.0°). It can also be seen that the other three methods (B3LYP, B3PW91 and MP2) also exhibit good applicability in predicting relatively accurate molecular structures. The above results show that DFT (B3P86, B3LYP, B3PW91) and MP2 methods are appropriate in studying the coupling systems.

Table 1. Calculated bond lengths (Å) and bond angles (°) of the four neutral monomers and the corresponding cations using different methods at the 6–311+G* basis set level

Parameter	B3P86	B3LYP	B3PW91	MP2	B3P86	B3LYP	B3PW91	MP2
	NH_3				NH_3^+			
N—H1	1.0127	1.0142	1.0131	1.0104	1.0394	1.0405	1.0396	1.0195
∠H2NH3	107.9	108.0	107.8	108.5	120.0	120.0	120.0	120.0
	NH_2CH_3				$NH_2CH_3^+$			
N—C	1.4557	1.4647	1.4577	1.4645	1.4071	1.4160	1.4097	1.4301
N—H1	1.0131	1.0144	1.0135	1.0122	1.0197	1.0209	1.0198	1.0188
∠CNH2	111.0	111.1	110.9	110.8	122.3	122.4	122.4	121.5
∠H1NH2	107.1	107.2	107.1	107.6	116.4	116.3	116.4	116.5
	$NH(CH_3)_2$				$NH(CH_3)_2^+$			
N—C1	1.4484	1.4568	1.4503	1.4558	1.4260	1.4354	1.4284	1.4378
N—H1	1.0131	1.0142	1.0133	1.0132	1.0190	1.0202	1.0191	1.0189
∠C1NC2	112.9	113.3	113.1	112.0	124.8	125.1	125.0	123.5
∠C2NH1	110.0	110.0	110.0	109.7	117.6	117.5	117.5	118.7
	$N(CH_3)_3$				$N(CH_3)_3^+$			
N—C1	1.4467	1.4544	1.4478	1.4527	1.4378	1.4479	1.4405	1.4475
∠C2NC3	111.4	111.7	111.5	111.5	120.0	120.0	120.0	120.0

Table 2. Calculated bond lengths (Å) and bond angles (°) of the four most stable complexes at the 6–311+G* basis set level

Parameter	B3P86	B3LYP	B3PW91	MP2	Parameter	B3P86	B3LYP	B3PW91	MP2[a]
$H_3NNH_3^+$					$(CH_3)_3NN(CH_3)_3^+$				
N1—N2	2.2092	2.2391	2.2178	2.1592	N1—N2	2.4848	2.5652	2.5288	2.3311
N1—H1	1.0131	1.0144	1.0132	1.0131	N1—C1	1.4485	1.4575	1.4500	1.4602
∠N2N1H1	105.3	105.3	105.4	105.9	∠N1N2C1	103.7	103.5	103.6	105.0
∠H1N1H2	113.3	113.3	113.2	112.8	∠C1N1C2	114.6	114.7	114.7	113.5
∠H1N1N2H5	60.0	60.0	60.0	60.0	∠C1N1N2C4	76.1	68.6	75.3	77.8
$CH_3NH_2NH_2CH_3^+$					$(CH_3)_2NHNH(CH_3)_2^+$				
N1—N2	2.2943	2.3317	2.3101	2.2106	N1—N2	2.3601	2.4117	2.3886	2.2464
N1—C1	1.4488	1.4583	1.4508	1.4618	N1—C1	1.4468	1.4572	1.4502	1.4598
N1—H1	1.0131	1.0144	1.0135	1.0146	N1—C2	1.4482	1.4558	1.4488	1.4605
N1—H2	1.0133	1.0141	1.0132	1.0145	N1—H1	1.0132	1.0141	1.0132	1.0205
∠N2N1C1	110.6	111.4	111.6	109.8	∠N2N1C1	109.1	109.5	109.6	110.0
∠N2N1H1	100.1	100.8	100.8	102.7	∠N2N1C2	106.5	106.6	106.6	105.8
∠N2N1H2	101.2	99.5	99.6	101.8	∠N2N1H1	93.7	93.0	93.0	97.0
∠C1N1H1	115.6	115.8	115.7	114.9	∠C1N1C2	117.4	117.6	117.5	116.3
∠C1N1H2	115.8	115.7	115.6	115.0	∠C2N1H1	113.6	113.5	113.5	112.9
∠H1N1H2	111.3	111.4	111.3	111.0	∠C1N1H1	113.6	113.5	113.5	112.9
∠C1N1N2C3	45.2	49.0	49.5	48.5	∠C1N1N2C3	146.8	139.8	139.5	148.1
∠C2N1N2H2	46.0	49.9	50.4	48.9	∠C1N1N2C4	146.8	139.8	139.6	148.1
∠H1N1N2C4	46.0	49.9	50.4	48.9	∠H1N1N2H8	146.8	139.2	139.0	146.9

[a] At the 6–31G* basis level.

Table 1 shows the regular variations of bond lengths (Å) and bond angles (degrees) in cations [NH_3^+, $NH_2CH_3^+$, $NH(CH_3)_2^+$, $N(CH_3)_3^+$] derived from the corresponding monomers [NH_3, NH_2CH_3, $NH(CH_3)_2$ or $N(CH_3)_3$]. In detail, when each neutral monomer loses an electron, becoming the corresponding monomer cation, the N—H bond length becomes long, the N—C bond length becomes short and the bond angles which are associated with the N atom become large. The results obtained by the B3P86 method show that the N—H bond length in NH_3 (1.0127 Å) is shorter than that in NH_3^+(1.0394 Å); the N—C bond length in NH_2CH_3 (1.4557 Å) is longer than that in $NH_2CH_3^+$ (1.4071 Å), but the N—H bond lengths are close to each other (1.0131 Å for the former vs 1.0197 Å for the latter). The N—C and N—H bond lengths in the other molecular pairs or at the other theoretical levels also exhibit similar regularity. The molecular structures of the four neutral monomers are all pyramidic, and the bond angles associated with the N atom are less than 120.0°. However, the molecular structures of the four cations are planar and the bond angles are 120.0° or almost 120.0°.

Geometric structures of the four coupling complexes [$H_3N\cdots NH_3^+$, $CH_3NH_2\cdots NH_2CH_3^+$, $(CH_3)_2HN\cdots NH(CH_3)_2^+$ and $(CH_3)_3N\cdots N(CH_3)_3^+$]

The bond lengths (Å) and bond angles (degrees) of $H_3N\cdots NH_3^+$, $CH_3NH_2\cdots NH_2CH_3^+$, $(CH_3)_2HN\cdots NH(CH_3)_2^+$ and $(CH_3)_3N\cdots N(CH_3)_3^+$ calculated by the B3P86, B3LYP, B3PW91 and MP2 methods at the 6–311+G* or 6–31G* basis set level are displayed in Table 2. The N1–N2 bond lengths in above four complexes are 2.2092, 2.2943, 2.3601 and 2.4848 Å, respectively, at the B3P86/6–311+G* level. The conclusion can be drawn that the more methyl substituents there are, the longer the N1–N2 bond length is. This may be attributed to the fact that the more methyl groups there are, the stronger the repulsive effect is. The N1–N2 bond lengths in above four complexes obtained with other three methods also exhibit similar characteristics. The C—N bond length in each of the four complexes is longer than that in the corresponding cation and is very close to that in the corresponding neutral monomer. In detail, the C—N bond lengths calculated with B3LYP method in NH_2CH_3, $NH_2CH_3^+$ and $CH_3H_2N\cdots NH_2CH_3^+$ are 1.4647, 1.4160 and 1.4583 Å, respectively; the C—N bond lengths in $NH(CH_3)_2$, $NH(CH_3)_2^+$ and $(CH_3)_2HN\cdots NH(CH_3)_2^+$ are 1.4568, 1.4354 and 1.4572 Å, respectively; and those of $N(CH_3)_3$, $N(CH_3)_3^+$ and $(CH_3)_3NN(CH_3)_3^+$ are 1.4544, 1.4479 and 1.4575 Å, respectively. The results of the other three methods are in agreement with the B3LYP method and show a similar variation.

With increase in methyl substituents, the ∠NNH and ∠NNC bond angles gradually become smaller, e.g. the ∠N1N2H bond angles of $H_3N\cdots NH_3^+$, $CH_3H_2N\cdots NH_2CH_3^+$ and $(CH_3)_2HN\cdots NH(CH_3)_2^+$ with the B3P86 method are 105.4°, 100.8° (99.6°) and 93.0°, respectively; the ∠N1N2C bond angles of $CH_3H_2N\cdots NH_2CH_3^+$, $(CH_3)_2HN\cdots NH(CH_3)_2^+$ and $(CH_3)_3N\cdots N(CH_3)_3^+$ are 111.6°, 109.6° (106.6°), 103.6°, respectively. The conclusion can be drawn that the repulsive effect becomes strong with increasing methyl substitution and the bond angle becomes smaller.

Table 3. Total charges of N centers of monomers and complexes at the 6–311+G* basis level

Species	B3P86	B3LYP	B3PW91	MP2
NH_3	−1.084	−1.048	−1.086	−1.111
NH_2CH_3	−0.652	−0.637	−0.645	−0.699
$NH(CH_3)_2$	−0.247	−0.251	−0.232	−0.314
$N(CH_3)_3$	0.301	0.176	0.217	0.121
NH_3^+	−0.847	−0.825	−0.846	−0.505
$NH_2CH_3^+$	−0.226	−0.223	−0.212	−0.175
$NH(CH_3)_2^+$	0.066	0.043	0.082	0.108
$N(CH_3)_3^+$	0.510	0.446	0.542	0.60
$NH_3NH_3^+$	−0.892	−0.850	−0.892	−0.918
$CH_3NH_2NH_2CH_3^+$	−0.487	−0.473	−0.471	−0.506
$(CH_3)_2NHNH(CH_3)_2^+$	−0.148	−0.158	−0.115	−0.551[a]
$(CH_3)_3NN(CH_3)_3^+$	0.342	0.341	0.414	0.570[a]

[a] At the 6–31G* basis level.

Total charge of N atom of the monomers and the complexes

The total charges of N centers in $NH_n(CH_3)_{3-n}$, $NH_n(CH_3)_{3-n}^+$ and $NH_n(CH_3)_{3-n}\cdots NH_n(CH_3)_{3-n}^+$ ($n = 0$–3) are listed in Table 3 calculated with the four methods at the 6–311+G* or 6–31G* basis set level. It can be seen that with the increasing methyl substitution, the total charges of N centers in the four neutral monomers, the four cations and the four complexes have similar variations. The total charge of the N center gradually changes from negative to positive with increase in methyl substitution. This phenomenon may be attributed to the stronger electron-attracting ability of C centers than that of the H atoms. In detail the B3P86 method yields total charges of N in NH_3, NH_2CH_3, $NH(CH_3)_2$ and $N(CH_3)_3$ of −1.084e, −0.652e, −0.247e and 0.301e, the total charges of N in the four corresponding cations are −0.847e, −0.226e, 0.066e and 0.510e and the total charges of N in the four complexes formed between the natural molecule and the corresponding cation are −0.892e, −0.487e, −0.148e and 0.342e, respectively. The total atomic charges of the four complexes (Table 3) also show equal delocalization of charge in the two parts. The above analysis reflects the effect of the substituent methyls on the total charges of N centers in the investigated systems. An increase in the number of methyl groups may cause the charge population to decrease over the active center N atoms. This tendency will significantly affect the electron transfer kinetic parameters, as mentioned below.

Relative stability of the four complexes

It is well known that the higher the stabilization energy, the more stable the molecule is. Table 4 shows the energies of the four monomers, the four cations and the four complexes and the stabilization energies of the four complexes. The stabilization energies of the four complexes obtained at the B3P86/6–311+G* level are 46.28, 34.37, 26.83 and 20.48 kcal mol^{-1}, respectively (1 kcal = 4.184 kJ). At the B3LYP/6–311+G* level, the calculated stabilization energies of the four complexes are 45.23, 33.41, 25.77 and 19.24 kcal mol, respectively. These data clearly indicate that the stability order of the four complexes is $H_3N\cdots NH_3^+ > CH_3H_2N\cdots NH_2CH_3^+ > (CH_3)_2\ HN\cdots NH(CH_3)_2^+ > (CH_3)_3N\cdots N(CH_3)_3^+$ and the interactions of the complexes are slightly weak.

'INVERSE SYMMETRY BREAKING' OF THE $(CH_3)_{3-n}H_nN\cdots NH_n(CH_3)_{3-n}^+$ ($n = 0$–3) COUPLING SYSTEMS

Figure 2 show the energy curves of the encounter complex with different contact distances $R_{N—N}$ of the

Table 4. Total energies E (a.u.) of monomers and complexes and binding energies, ΔE (kcal mol^{-1}), at the 6–311+G* basis level

Parameter	B3P86	B3LYP	B3PW91	MP2
$E(NH_3)$	−56.7516742	−56.5728243	−56.5499653	−56.386091
$E(NH_3^+)$	−56.3595506	−56.1999352	−56.1794125	−56.027684
$E(H_3NNH_3^+)$	−113.1849704	−112.8448471	−112.8005984	−112.4731332
ΔE	46.28	45.23	44.69	37.25
$ET(NH_2CH_3)$	−96.2078892	−95.883616	−95.8457376	−95.5518813
$ET(NH_2CH_3^+)$	−95.8597822	−95.5549952	−95.5187626	−95.2285204
$ET(CH_3H_2NNH_2CH_3^+)$	−192.1224421	−191.4918586	−191.4169251	−190.8303262
$\Delta E(\ CH_3H_2NNH_2CH_3^+)$	34.37	33.41	32.90	31.33
$ET(N(CH_3)_3)$	−135.6688397	−135.1988832	−135.1459176	−134.6652982[a]
$ET(N(CH_3)_3)^+$	−135.3478216	−134.8976356	−134.8460492	−134.3740755[a]
$ET((CH_3)_2HNNH(CH_3)_2^+)$	−271.0594166	−270.1375842	−270.0320416	−269.0862262[a]
$\Delta E((CH_3)_2HNNH(CH_3)_2^+)$	26.83	25.77	25.15	29.40[a]
$ET(N(CH_3)_3)$	−175.1327842	−174.516451	−174.4486993	−173.8285982[a]
$ET(N(CH_3)_3^+)$	−174.8294027	−174.2334865	−174.1666223	−173.5534749[a]
$ET((CH_3)_3NN(CH_3)_3^+)$	−349.9948217	−348.7805923	−348.6443523	−347.4239617[a]
$\Delta E((CH_3)_3NN(CH_3)_3^+)$	20.48	19.24	18.22	26.28[a]

[a] At the 6–31G* basis level.

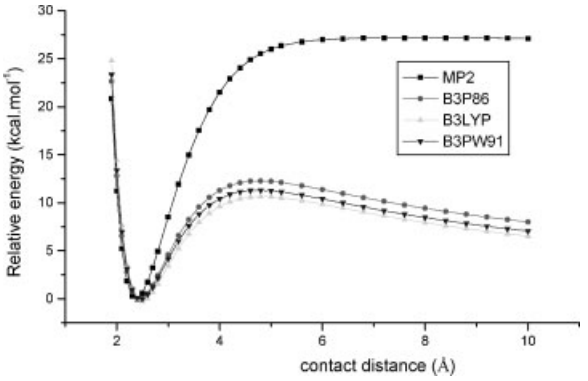

Figure 2. Relative energy (kcal mol^{-1}) for the activated state of the coupling system $H_3N\cdots NH_3^+$ at different contact distances $R_{N—N}$ (Å) obtained using different methods

$H_3N\cdots NH_3^+$ coupling system. The contact distance ($R_{N—N}$) corresponding to the minimum energy in the coupling system is defined as the zero point. It can be seen that the zero point of the $H_3N\cdots NH_3^+$ coupling systems is 2.40 Å.

Figure 2 shows an abnormal behavior in the energy curves obtained with the DFT methods (B3LYP, B3P86, B3PW91) for $H_3N\cdots NH_3^+$ system. The total energy of the system decreases to the zero point and then increases with increasing contact distance from about 2.0 to 5.0 Å. Obviously, this behavior is normal. However, along with the increase in the contact distance (from about 5.0 to 10 Å), the abnormal behavior appears for DFT methods. The main abnormal features can be depicted as the following two aspects. One is that the larger the contact distance, the lower the energy is and the other is that the positive charge and the spin of the radical cation are delocalized evenly in the two fragments, and are independent of the contact distance. It is well known that for a real system it should be the case that when the $R_{N—N}$ is large enough, each of the energies of the complex is the sum of the energies of the monomer and its corresponding monomer cation, and the positive charge and the spin of the radical cations are not delocalized evenly in the two fragments. Hence the results of energy curves with DFT methods are definitely unreasonable. This abnormal behavior (named the 'inverse symmetry breaking' problem) was first reported in an important paper by Bally and Sastry in 1997.[12] Lately the 'inverse symmetry breaking' problem has been mentioned[26,27] in the results obtained by DFT methods for radical ions with two equivalent fragments. For the MP2 method, the energy curve exhibits the normal behavior. The energy curves calculated by DFT methods and the MP2 method for the $CH_3H_2N\cdots NH_2CH_3^+$, $(CH_3)_2HN\cdots NH(CH_3)_2^+$ and $(CH_3)_3N\cdots N(CH_3)_3^+$ coupling systems are similar to those for the $H_3N\cdots NH_3^+$ coupling system [in order to express the character in a compact way, the figures for the energy curves calculated by DFT methods and the MP2 method for the $CH_3H_2N\cdots NH_2CH_3^+$, $(CH_3)_2HN\cdots NH(CH_3)_2^+$, $(CH_3)_3N\cdots N(CH_3)_3^+$ coupling systems are not shown in this paper]. This phenomenon has indicated that although DFT methods can yield results accurate enough for the geometric parameters and the various energy quantities of these molecular complexes and their monomer ions at the equilibrium geometries, they cannot predict correct dissociation energy curves. Of course, the complete active space SCF method (CASSCF) can also correctly predict the dissociation behavior of these kinds of the complexes, but it needs a large computer source, and it is even impossible to perform the calculations regarding the larger systems using this method. Many investigations of other small systems and our preliminary calculations on the $H_3N\cdots NH_3^+$ system indicate that the MP2 method is well applied not only to equilibrium systems but also to coupling systems far from equilibrium.[28] Therefore, the MP2 method was chosen to scan the energy minimum pathway for the dissociation along the contact distance in order to investigate the electron transfer reactivity of the $(CH_3)_{3-n}H_nN\cdots NH_n(CH_3)_{3-n}^+$ coupling system.

ACTIVATION ENERGY

Activation energy is the energy barrier of an electron transfer reaction. The greater the activation energy, the more difficult the electron transfer reaction is. The exponential relationship between the electron transfer rate and the activation energy can be seen from Eqn (9).

Figure 3 and Tables 5 and 6 demonstrate the contact distance dependence of the activation energy $E_a(R_{N—N})$ for the four coupling systems. It can be seen that the activation energies first decrease and then increase with increasing contact distance $R_{N—N}$ in four investigated coupling systems. From Fig. 3 it can be seen that the activation energies for the four coupling complexes exhibit the same characteristic variations. Actually, these observed regular variations for the activation energy

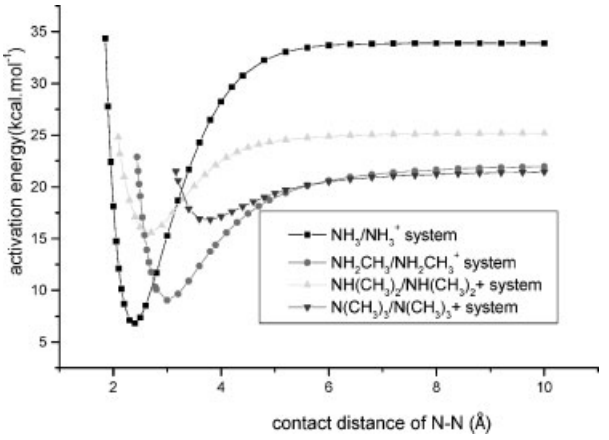

Figure 3. Contact distance $R_{N—N}$ (Å) dependence of the activation energy $E_a(R_{N—N})$ (kcal mol^{-1}) for the four coupling systems obtained at the MP2/6–311+G* level

should be attributed to the changes in geometry parameters, such as bond lengths, bond angles and dihedral angles. In the case of the $NH_3\cdots NH_3^+$ coupling system, it is known that substantial changes in the reactant geometries should occur for the ∠HNH bond angle before and after ET. For NH_3, before ET, the ∠HNH bond angle is about 108.0°. However, after ET, this bond angle is about 120.0°. Changes in the other geometric parameters, such as bond angles and dihedral angles, are not evident. Obviously, this observation indicated that ET may significantly change ∠HNH. Equation (12) suggests that R_1^* should be equal to R_2^* at the given contact distance. Using the minimization method, the corresponding minimum activation energy and the geometric parameters of the complex at the activated states may be obtained in which the more obvious change lies in the ∠HNH bond angle becoming 120.0°. The other three coupling systems can also be analyzed similarly to the NH_3/NH_3^+ coupling system. In detail, for the $H_3N\cdots\ NH_3^+$ coupling system, the activation energy decreases sharply from 34.36 to 6.81 kcal mol^{-1} with the corresponding contact distance increasing from 1.85 to 2.40 Å, and the activation energy still increases at other contact distances from 2.40 to 10.0 Å. For the $CH_3H_2N\cdots\ NH_2CH_3^+$ coupling system, the activation energy also decreases from 22.89 to 9.04 kcal mol^{-1} when the corresponding contact distance increases from 2.44 to 3.0 Å. For the other two coupling systems $[(CH_3)_2HN\cdots\ NH(CH_3)_2^+$ and $(CH_3)_3N\cdots N(CH_3)_3^+]$, the activation energies decrease gradually compared with the other two systems. For the $(CH_3)_2HN\cdots NH(CH_3)_2^+$ coupling system, the activation energy decreases from 24.78 to 15.59 kcal mol^{-1} when the contact distance increases from 2.09 to 2.70 Å. For the $(CH_3)_3N\cdots N(CH_3)_3^+$ coupling system, the activation energy decreases from 21.49 to 16.88 kcal mol^{-1} with the contact distance increasing from 3.16 to 3.70 Å. When the contact distance increases from the zero point to 10.0 Å, the activation energies increase continuously.

The above results show that the minimum active energy in each energy curve increases as the number of substituent methyl groups increases, and suggest that the rate of the electron transfer reaction decreases in the order $H_3N\cdots NH_3^+ > CH_3H_2N\cdots NH_2CH_3^+ > (CH_3)_2HN\cdots NH(CH_3)_2^+ > (CH_3)_3N\cdots N(CH_3)_3^+$.

Coupling matrix element

From Eqn (7), we can draw the conclusion that a larger coupling matrix element corresponds to a faster rate of the electron transfer. The dependence of the coupling matrix elements (H_{if}) on the contact distance $R_{N—N}$ is demonstrated in Fig. 4 and Tables 5 and 6 for the four coupling systems. It can be seen that the coupling matrix elements of the four coupling systems exhibit similar variations, namely, the coupling matrix element first increases and then decreases with increase in the contact distance.

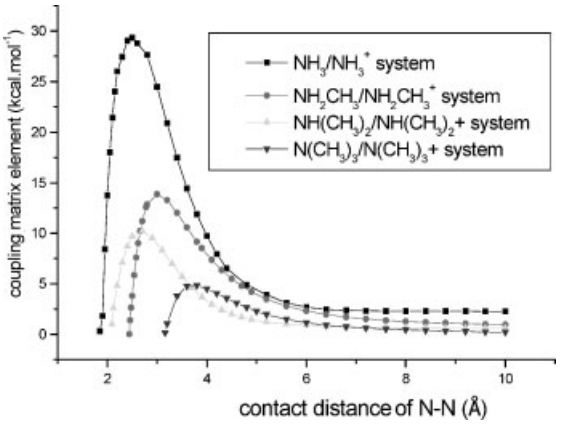

Figure 4. Contact distance $R_{N—N}$ (Å) dependence of the coupling matrix element $H_{if}(R_{N—N})$ (kcal mol^{-1}) for the four coupling systems obtained at the MP2/6–311+G* level

For the $H_3N\cdots NH_3^+$ coupling system, the coupling matrix element increases progressively from 1.82 to 29.36 kcal mol^{-1} when the contact distance increases from 1.85 to 2.40 Å. The coupling matrix elements of $CH_3H_2N\cdots NH_2CH_3^+$ are always lower than those of $H_3N\cdots NH_3^+$ in the investigated range between 2.0 and 10.0 Å. In detail, the coupling matrix element increases sharply from 1.39 to 13.87 kcal mol^{-1} when the corresponding contact distance increases from 2.46 to 3.0 Å. For the $(CH_3)_2HN\cdots NH(CH_3)_2^+$ coupling system, the coupling matrix element increases from 0.99 to 10.19 kcal mol^{-1} with the corresponding contact distance increasing from 2.09 to 2.70 Å. In the case of the $(CH_3)_3N\cdots N(CH_3)_3^+$ coupling system, the coupling matrix element is only 0.14 kcal mol^{-1} at a contact distance of 3.16 Å, but when the contact distance is close to 3.70 Å, the coupling matrix element becomes 4.86 kcal mol^{-1}.

These results indicate that the dependences of the coupling matrix elements on the contact distances of the four coupling systems have similar characteristics. Furthermore, the maximum coupling matrix elements in the investigated systems decrease with increasing methyl substitution. The ET reaction of the $H_3N\cdots NH_3^+$ coupling system occurs chiefly in a range of contact distances where $1.9\ Å < R_{N—N} < 4.0\ Å$. For the three other coupling systems $[CH_3H_2N\cdots NH_2CH_3^+$, $(CH_3)_2HN\cdots NH(CH_3)_2^+$ and $(CH_3)_3N\cdots N(CH_3)_3^+]$, the ET reactions occur chiefly over a range of contact distances where $2.5\ Å < R_{N—N} < 5.0\ Å$, $2.1\ Å < R_{N—N} < 5.0\ Å$ and $3.2\ Å < R_{N—N} < 6.0\ Å$, respectively. Therefore, it can be concluded that in the region of the above contact distance H_{if} changes rapidly and the values are significantly larger than those in the other regions. These results also show the strong coupling effect between the donor and the acceptor, which dominates the electron transfer reaction.

Actually, the observed regular variation of H_{if} with the contact distance for these four coupling systems is

closely related to the bonding interaction between the donor and acceptor in each coupling pair. Obviously, the considerable bonding interaction between the donor and the acceptor may favor the electron transfer. The natural bond orbital and molecular orbital population analysis has indicated that the main binding interaction between the donor and the acceptor is that between the hybrid (s, p) orbitals of the donor and the acceptor. For the $H_3N\cdots NH_3^+$ system, the electronic configuration is $(1a_{2u})^2(1a_{1g})^2(2a_{1g})^2(2a_{2u})^2(1e_u)^4(1e_g)^4(3a_{1g})^2\ (3a_{2u})^1$. Inspection of the molecular orbitals indicates that $1a_{2u}$ and $1a_{1g}$ orbitals are obviously the two lone-pair orbitals of two N atoms, and $2a_{1g}$ and $2a_{2u}$ correspond to the bonding and the antibonding interaction between two 2s orbitals of two N atoms. Their net bonding contributions to the N—N bond is almost equal to zero, so these two $2a_{1g}$ and $2a_{2u}$ orbitals are essentially two lone-pair orbitals. Obviously, $1e_u$ and $1e_g$ orbitals are two groups of degenerate orbitals, which describe all N—H bonding interactions. The remaining molecular orbitals are $3a_{1g}$ and $3a_{2u}$ orbitals, which are the N—N bonding orbital and the antibonding orbital, formed by their hybrid (s, p) atomic orbitals. The $3a_{1g}$ orbital is doubly occupied, whereas $3a_{2u}$ is singly occupied. Similarly for the $CH_3H_2N\cdots NH_2CH_3^+$, $(CH_3)_2HN\cdots NH(CH_3)_2^+$ and $(CH_3)_3N\cdots N(CH_3)_3^+$ coupling systems, the effective bonding interaction between two NR_3 molecular fragments are one a' and one a'', in which the former is doubly occupied and the latter is singly occupied. Inspection of the bonding nature of these two a' and a'' orbitals for the $H_3N\cdots NH_3^+$, $CH_3H_2N\cdots NH_2CH_3^+$, $(CH_3)_2HN\cdots NH(CH_3)_2^+$ and $(CH_3)_3N\cdots N(CH_3)_3^+$ coupling systems indicates that a' is the bonding orbital and a'' is the antibonding orbital. Actually, they also correspond to those reduced from $3a_{1g}$ and $3a_{2u}$ when the symmetry goes down. Hence the main orbitals describing the coupling interaction between $NH_n(CH_3)_{3-n}$ and $NH_n(CH_3)_{3-n}^+$ are these two orbitals. Therefore, the overall bonding interaction is that the bonding is slightly greater than the antibonding, indicating that the net coupling interaction is one of bonding. Actually, both of these two orbitals lie in the frontier orbital zone and their energy levels are relatively high. The overall bonding interaction should also be relatively smaller than that of the a' orbital owing to the contribution from the a'' orbital. Figure 5 clearly displays the orbital coupling interaction case for a' and a'' of these four coupling systems. In addition, for these ET systems, the N···N contact distances between two molecular fragments are ca. 2.2–2.5 Å, significantly longer than the common N—N bond length in other amine compounds. All these analyses indicate that the coupling interaction between $NH_n(CH_3)_{3-n}$ and $NH_n(CH_3)_{3-n}^+$ should be relatively weak.

Comparison of a' and a'' of the four coupling systems can clarify the relative coupling strength between the N···N interactions in four coupling systems. At the

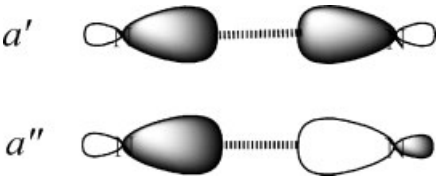

Figure 5. Main coupling orbitals between $NH_n(CH_3)_{3-n}$ and $NH_n(CH_3)_{3-n}$

N—N contact distance of the four stable complexes, we determined the molecular orbital and the natural orbitals for four coupling systems. The orbital levels in $H_3N\cdots NH_3^+$ coupling system are −0.57403 a.u. for the a_{1g} and −0.35597 a.u. for the a_{2u} orbital, whereas those in the $CH_3H_2N\cdots NH_2CH_3^+$, $(CH_3)_2HN\cdots NH(CH_3)_2^+$ and $(CH_3)_3N\cdots N(CH_3)_3^+$ coupling systems are −0.49406 a.u., −0.45230 a.u. and −0.42431 a.u. for a' orbitals and −0.32706 a.u., −0.31009 a.u. and − 0.30475 a.u. for a'' orbitals at the B3P86/6–311+G* level, respectively. From viewpoint of orbital energy levels, these data seem to indicate that the N···N coupling interaction decreases in the order $H_3N\cdots NH_3^+ > CH_3H_2N\cdots NH_2CH_3^+ > (CH_3)_2HN\cdots NH(CH_3)_2^+ > (CH_3)_3N\cdots N(CH_3)_3^+$. Moreover, the overall coupling strength should be determined by all factors. If we consider the net energy contributions by filling three electrons in these a' and a'' orbitals, we can find another regularity. The bonding orbital, a', and the antibonding orbital, a'', may be viewed as the molecular orbitals formed by direct coupling between the sp^n hybrid orbital of $NH_n(CH_3)_{3-n}$ and that of the $NH_n(CH_3)_{3-n}^+$ fragment, so the net bonding contribution to the coupling system should be that obtained by deducting the antibonding contribution from the bonding contribution. They are −0.79209 a.u. for the $H_3N\cdots NH_3^+$ coupling system, −0.66106 a.u. for the $CH_3H_2N\cdots NH_2CH_3^+$ coupling system, −0.59451 a.u. for the $(CH_3)_2HN\cdots NH(CH_3)_2^+$ coupling system and −0.54387 a.u. for the $(CH_3)_3N\cdots N(CH_3)_3^+$ coupling system. Obviously, these two sets of data reflect the relative coupling strength, namely that the coupling interaction of the four coupling systems decreases in the order $H_3N\cdots NH_3^+ > CH_3H_2N\cdots NH_2CH_3^+ > (CH_3)_2HN\cdots NH(CH_3)_2^+ > (CH_3)_3N\cdots N(CH_3)_3^+$. This analysis has further demonstrated the above contact distance dependence of the coupling matrix elements of four coupling systems: in the range from 2.0 to 4.0 Å, the H_{if} of the $H_3N\cdots NH_3^+$ coupling system is larger than those of the other three coupling systems at the same contact distance. This also indicates that an increase in electron-attracting groups may reduce the coupling interaction strength between the $NH_n(CH_3)_{3-n}$ and $NH_n(CH_3)_{3-n}^+$ ($n = 1$–3) moieties.

Natural bond orbital (NBO)[29] analysis also reflected similar coupling characteristics. For the $H_3N\cdots NH_3^+$ coupling system, each molecular fragment uses an $sp^{10.11}$ hybrid orbital to interact with the other one, forming a natural bonding orbital, and at the same time,

Table 5. Contact distance, $R_{N—N}$ (Å), of activation energy, E_a (kcal mol^{-1}), coupling matrix element H_{if}(kcal mol^{-1}) and electron transfer rate, log [k_{et} (s^{-1})] of $H_3N\cdots NH_3^+$ and $CH_3H_2N\cdots NH_2CH_3^+$ coupling systems at the MP2/6–311+G* level

$NH_3\cdots NH_3^+$ coupling system				$NH_2CH_3\cdots NH_2CH_3^+$ coupling system			
$R_{N—N}$	E_a	H_{if}	Log k_{et}	$R_{N—N}$	E_a	H_{if}	Log k_{et}
1.85	34.36	1.82	−17.55	2.44	22.89	0.02	−12.89
1.90	27.77	8.41	−11.34	2.46	21.52	1.39	−8.27
1.95	22.42	13.75	−6.95	2.48	20.26	2.65	−6.78
2.00	18.14	18.03	−3.53	2.50	19.11	3.81	−5.60
2.05	14.75	21.42	−0.85	2.54	17.06	5.85	−3.70
2.10	12.12	24.05	1.22	2.58	15.33	7.58	−2.19
2.15	10.14	26.03	2.78	2.62	13.90	9.01	−0.97
2.20	8.70	27.47	3.91	2.66	12.71	10.20	0.03
2.25	7.72	28.45	4.69	2.70	11.73	11.18	0.85
2.30	7.12	29.05	5.16	2.78	10.33	12.58	2.00
2.35	6.90	29.34	5.39	2.80	10.08	12.83	2.21
2.40	6.81	29.36	5.41	2.90	9.26	13.65	2.88
2.45	7.00	29.17	5.25	3.00	9.04	13.87	3.06
2.50	7.37	28.80	4.96	3.10	9.21	13.70	2.93
2.60	8.51	27.66	4.06	3.20	9.64	13.27	2.57
2.80	11.71	24.46	1.54	3.30	10.23	12.68	2.09
3.00	15.28	20.89	−1.27	3.40	10.90	12.01	1.53
3.20	18.69	17.48	−3.96	3.50	11.62	11.29	0.93
3.40	21.71	14.46	−6.37	3.60	12.35	10.56	0.33
3.60	24.29	11.88	−8.46	3.70	13.07	9.85	−0.27
3.80	26.46	9.71	−10.24	3.80	13.75	9.16	−0.84
4.00	28.23	7.94	−11.73	3.90	14.39	8.51	−1.39
4.20	29.65	6.52	−12.95	4.00	15.00	7.91	−1.90
4.40	30.76	5.41	−13.94	4.10	15.57	7.35	−2.39
4.60	31.61	4.56	−14.71	4.20	16.09	6.82	−2.85
4.80	32.25	3.93	−15.31	4.30	16.57	6.34	−3.27
5.00	32.72	3.46	−15.77	4.50	17.41	5.50	−4.02
5.20	33.06	3.11	−16.12	4.70	18.12	4.79	−4.67
5.40	33.30	2.87	−16.37	4.90	18.72	4.19	−5.23
5.60	33.47	2.69	−16.56	5.20	19.42	3.49	−5.91
5.80	33.61	2.56	−16.69	5.60	20.11	2.80	−6.62
6.00	33.70	2.47	−16.79	6.00	20.60	2.34	−7.14
6.40	33.81	2.37	−16.91	6.40	20.94	1.97	−7.54
6.80	33.85	2.32	−16.96	6.80	21.20	1.71	−7.85
7.20	33.87	2.30	−16.98	7.20	21.39	1.53	−8.09
7.60	33.87	2.30	−16.98	7.60	21.54	1.38	−8.29
8.00	33.87	2.30	−16.98	8.00	21.65	1.26	−8.45
8.40	33.88	2.29	−16.99	8.40	21.74	1.17	−8.58
8.80	33.88	2.29	−16.99	8.80	21.81	1.11	−8.68
9.20	33.89	2.28	−16.70	9.20	21.87	1.04	−8.77
9.60	33.89	2.28	−17.00	9.60	21.91	1.00	−8.84
10.0	33.89	2.28	−17.00	10.00	21.96	0.96	−8.92

each use three $sp^{2.30}$ hybrid orbitals to interact with three H 1s atomic orbitals, forming three N—H bonds. The electron occupation for this N—N natural orbital is 0.998e and its energy level is −0.61836 a.u. at the B3P86/6–311+G* level.

All the analyses below are at the B3P86/6–311+G* level. For the $CH_3H_2N\cdots NH_2CH_3^+$ coupling system, the N hybrid orbitals used for forming direct N···N coupling are two $sp^{13.23}$ orbitals, those for forming one N—C bond are $sp^{1.67}$ orbitals, and the others for forming two N—H bonds are $sp^{2.59}$, $sp^{2.60}$ orbitals, respectively. The energy level of the formed N···N natural bond orbital is −0.55774 a.u. and its occupation is 0.984e. For the $(CH_3)_2HN\cdots NH(CH_3)_2^+$ coupling system, the N hybrid orbitals used for forming direct N···N coupling are two $sp^{16.46}$ orbitals, those for forming one N—H bond are $sp^{2.98}$ orbitals and the others for forming two N—C bonds are $sp^{1.88}$, $sp^{1.90}$orbitals, respectively. The energy level of the formed N···N natural bond orbital is −0.51495 a.u. and its occupation is 0.965e. In the case of the $(CH_3)_3N\cdots N(CH_3)_3^+$ coupling system, the N hybrid orbitals used for forming direct N···N coupling are two $sp^{19.35}$ orbitals and those for forming N—C bonds are $sp^{2.15}$ orbitals. The energy level of the formed N···N natural bond orbital is −0.47873 a.u. and its occupation is 0.944e.

The electronic energies in their natural orbitals (−0.61729 a.u. for the $H_3N\cdots NH_3^+$ coupling system,

Table 6. Contact distance, $R_{N—N}$ (Å), of activation energy E_a (kcal mol^{-1}) coupling matrix element, H_{if} (kcal mol^{-1}), and electron transfer rate, log [k_{et} (s^{-1})] of the $(CH_3)_2HN\cdots NH(CH_3)_2^+$ and $(CH_3)_3N\cdots N(CH_3)_3^+$ coupling systems at the MP2/6–31G* level

$NH(CH_3)_2\cdots NH(CH_3)_2^+$ coupling system				$N(CH_3)_3\cdots N(CH_3)_3^+$ coupling system			
$R_{N—N}$	E_a	H_{if}	Log k_{et}	$R_{N—N}$	E_a	H_{if}	Log k_{et}
2.09	24.78	0.99	−10.99	3.16	21.49	0.14	−10.23
2.12	23.19	2.59	−8.97	3.18	21.03	0.61	−8.62
2.2	20.95	4.83	−6.76	3.20	20.60	1.03	−7.84
2.3	18.69	7.08	−4.75	3.30	18.92	2.71	−5.76
2.5	16.10	9.67	−2.55	3.40	17.85	3.78	−4.67
2.7	15.59	10.19	−2.12	3.50	17.21	4.42	−4.06
2.9	16.27	9.51	−2.69	3.60	16.77	4.74	−3.75
3.1	17.47	8.31	−3.71	3.70	16.88	4.86	−3.65
3.3	18.80	6.97	−4.85	3.80	16.81	4.82	−3.68
3.5	20.07	5.71	−5.96	3.90	16.93	4.70	−3.80
3.7	21.18	4.59	−6.98	4.00	17.12	4.51	−3.98
3.9	22.10	3.68	−7.85	4.10	17.35	4.28	−4.19
4.1	22.82	2.95	−8.58	4.30	17.83	3.80	−4.65
4.3	23.37	2.40	−9.17	4.50	18.32	3.31	−5.13
4.5	23.79	1.99	−9.64	4.60	18.55	3.08	−5.37
4.7	24.09	1.69	−10.01	4.80	18.98	2.65	−5.82
4.9	24.31	1.46	−10.30	5.00	19.35	2.28	−6.22
5.2	24.55	1.23	−10.62	5.20	19.67	1.96	−6.59
5.6	24.75	1.03	−10.92	5.60	20.16	1.47	−7.21
6.0	24.88	0.90	−11.14	6.00	20.49	1.14	−7.68
6.4	24.97	0.80	−11.31	6.40	20.72	0.91	−8.05
6.8	25.03	0.74	−11.42	6.80	20.90	0.74	−8.35
7.2	25.09	0.69	−11.52	7.20	21.02	0.61	−8.61
7.6	25.12	0.66	−11.59	7.60	21.12	0.51	−8.84
8.0	25.14	0.63	−11.64	8.00	21.20	0.43	−9.05
8.4	25.16	0.62	−11.68	8.40	21.26	0.37	−9.23
8.8	25.17	0.60	−11.70	8.80	21.32	0.31	−9.42
9.2	25.19	0.59	−11.73	9.20	21.36	0.27	−9.59
9.6	25.19	0.58	−11.75	9.60	21.39	0.24	−9.72
10.0	25.20	0.58	−11.76	10.00	21.43	0.20	−9.86

−0.54869 a.u. for the $CH_3H_2N\cdots NH_2CH_3^+$ coupling system, −0.49693 a.u. for the $(CH_3)_2HN\cdots NH(CH_3)_2^+$ coupling system and −0.54387 a.u. for $(CH_3)_3N\cdots N(CH_3)_3^+$ coupling system) show that the coupling interaction of the four coupling systems decreases in the order $NH_3\cdots NH_3^+ > NH_2CH_3\cdots NH_2CH_3^+ > NH(CH_3)_2\cdots NH(CH_3)_2^+ > N(CH_3)_3\cdots N(CH_3)_3^+$. Moreover, from the overall contributions of the electronic energies and the nuclear repulsion energies in which the effective repulsion energies of the four coupling systems decreases in the order $N(CH_3)_3\cdots N(CH_3)_3^+ > NH(CH_3)_2\cdots NH(CH_3)_2^+ > NH_2CH_3\cdots NH_2CH_3^+ > NH_3\cdots NH_3^+$, we can easily predict that the coupling interaction of the four coupling systems decreases in the order $NH_3\cdots NH_3^+ > NH_2CH_3\cdots NH_2CH_3^+ > NH(CH_3)_2\cdots NH(CH_3)_2^+ > N(CH_3)_3\cdots N(CH_3)_3^+$.

The above analysis has explained the overall relative coupling strength among the four coupling systems. Let us now consider the dependence of the coupling strength on the contact distance. It can be understood from the following analysis. The above analysis also implies from another viewpoint the coupling mode between donor and acceptor, viz., for every coupling pair, they use their (s, p) hybrid orbitals to yield the direct through-bond coupling with each other. Hence the orbital overlap and repulsion between the donor and the acceptor consists of the main factors influencing the coupling variation trend along the contact distance. When the contact distance between the donor and the acceptor is large, the direct orbital interaction is small, and therefore the coupling matrix element should be small. Along with the decrease in the contact distance, the direct orbital interaction is gradually strengthened, so the coupling matrix element gradually becomes large. At the same time, this direct coupling interaction also gradually lowers the total energy of the complex, resulting in the coupling system becoming more stable. However, when the contact distance reaches a definite value, the coupling matrix element begins to be reduced along with the decrease in the contact distance, and a maximum appears for the coupling matrix. This phenomenon should be attributed to the large repulsion interaction between the donor and the acceptor when the contact distance is small. Although the shorter contact distance is more favorable to the bonding interaction, the molecular orbitals have definite shapes; when the contact distance is reduced to some smaller value, the overall

orbital overlap interaction will become small because in this contact distance range, the bonding overlap is gradually decreased and the antibonding overlap is gradually increased along with the decrease in the contact distance. Together with the sharply increased repulsion interaction, these factors cause the overall coupling matrix element between the donor and the acceptor to decrease in the smaller contact distance range. Therefore, the dependence of the coupling matrix element exhibits a parabola with a maximum.

Electron transfer rate

Equation (7) shows that there are two main contributions to the rate of electron transfer $k_{et}(R_{N—N})$ at different contact distances: the coupling matrix element $H_{if}(R_{N—N})$ and the Franck–Condon factor $FC(R_{N—N})$. FC depends on the activation energy $E_N(R_{N—N})$ and the reorganization energy $E_\lambda(R_{N—N})$. For the self-exchange ET reaction, Marcus[30] established a relation that the activation energy $E_a(R_{N—N})$ equals approximately one-quarter of the reorganization energy $E_\lambda(R_{N—N})$. Hence we can draw the conclusion that the ET rates at different contact distances depend on activation energy $E_a(R_{N—N})$ and coupling matrix element $H_{if}(R_{N—N})$. Figure 6 and Tables 5 and 6 show the contact distance $R_{N—N}$ (Å) dependence of the ET rate $\log[k_{et}(R_{N—N})\ (s^{-1})]$ of the four coupling systems. From the factors affecting the ET rate and Fig. 6, we can see that the ET rates at different contact distances of the four coupling systems exhibit similar variations. With the contact distance changing from about 2.0 to 10.0 Å, the ET rate first increases, reaches a maximum and then decreases.

In the case of the ET reaction of the $H_3N\cdots NH_3^+$ coupling system, when the contact distance is 2.4 Å, the ET rate tends to a maximum constant value ($2.53\times 10^5\ s^{-1}$). At this contact distance (where $R_{N—N}$ is about 2.4 Å), the reactive coupling system has the lowest activation energy ($6.81\ kcal\ mol^{-1}$) and the largest coupling matrix element ($29.36\ kcal\ mol^{-1}$). Above a 2.4 Å contact distance, k_{et} rapidly decreases as $R_{N—N}$ increases. For the ET reaction of the $CH_3H_2N\cdots NH_2CH_3^+$ coupling system, the ET rate is slower than that of the $H_3N\cdots NH_3^+$ coupling system. The most favorable contact distance for ET is 3.0 Å, where the ET rate tends to a maximum constant value ($1.16\times 10^3\ s^{-1}$), and the corresponding activation energy for the coupling system is the lowest, being only $9.04\ kcal\ mol^{-1}$, and the corresponding coupling matrix element is the largest ($13.87\ kcal\ mol^{-1}$), compared with those values in the other contact distance ranges. Above a 3.0 Å contact distance, k_{et} rapidly decreases with $R_{N—N}$ increase. However, the most favorable contact distance for the ET reaction of the $(CH_3)_2HN\cdots NH(CH_3)_2^+$ coupling system is 2.7 Å, where the ET rate tends to the maximum constant value ($7.55\times 10^{-3}\ s^{-1}$) and the corresponding activation energy for the coupling system is the lowest, being only $15.59\ kcal\ mol^{-1}$, and the corresponding coupling matrix element is the largest ($10.19\ kcal\ mol^{-1}$), compared with the values in the other contact distance ranges. Above a 2.7 Å contact distance, k_{et} rapidly decreases with $R_{N—N}$ increase and the ET rate of the $(CH_3)_2HN\cdots NH(CH_3)_2^+$ coupling system is less than that of the $CH_3H_2N\cdots NH_2CH_3^+$ coupling system.

For the ET reaction of the $(CH_3)_3N\cdots N(CH_3)_3^+$ coupling system, the ET rate is less than that of the $(CH_3)_2HN\cdots NH(CH_3)_2^+$ coupling system. The most favorable contact distance for ET is about 3.7 Å, where the ET rate tends to the maximum constant value ($2.25\times 10^{-4}\ s^{-1}$) and the corresponding activation energy for the coupling system is the lowest, being only $16.77\ kcal\ mol^{-1}$, and the corresponding coupling matrix element is the largest ($4.86\ kcal\ mol^{-1}$), compared with those in the other contact distance ranges. Above a 3.0 Å contact distance, k_{et} rapidly decreases with $R_{N—N}$ increase. When $R_{N—N} > 4.0$ Å for the $H_3N\cdots NH_3^+$ coupling system, $R_{N—N} > 5.0$ Å for the $CH_3H_2N\cdots NH_2CH_3^+$ and $(CH_3)_2HN\cdots NH(CH_3)_2^+$ coupling systems and $R_{N—N} > 6.0$ Å for the $(CH_3)_3N\cdots N(CH_3)_3^+$ coupling system, k_{et} gradually decays with the increase in the contact distances for the four coupling systems. Moreover, the coupling systems have a high activation energy barrier and a small coupling matrix element compared with those for the other contact distances and the variations of the contact dependence of k_{et}, the activation energy and the coupling matrix element tend to be straight lines with those contact distances of the ET reactions of the four coupling systems.

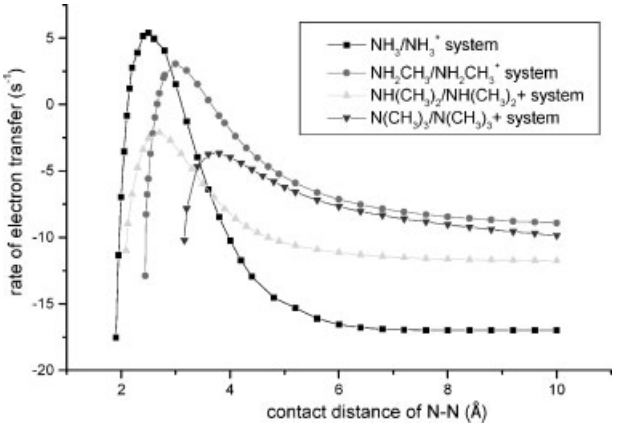

Figure 6. Contact distance $R_{N—N}$ (Å) dependence of the electron transfer rates (s^{-1}) for the four coupling systems obtained at the MP2/6–311+G* level

CONCLUSION

The geometries of $NH_n(CH_3)_{3-n}$, $NH_n(CH_3)_{3-n}^+$ ($n=$ 0–3) and their corresponding coupling complexes $[NH_n(CH_3)_{3-n}\cdots NH_n(CH_3)_{3-n}^+$ ($n=0$–3)] formed between the neutral monomers and cations were determined

using DFT and second-order Møller-Plesset perturbation theory (MP2) *ab initio* methods at the 6–311+G* basis set level. The results show that the stabilization energies of the four encounter complexes decrease with increase in the substituent methyl groups owing to the repulsive effect of substituent methyl groups, and the order of stability is $H_3N\cdots NH_3^+ > CH_3H_2N\cdots NH_2CH_3^+ > (CH_3)_2HN\cdots NH(CH_3)_2^+ > (CH_3)_3N\cdots N(CH_3)_3^+$.

The contact distance dependences of the activation energy, the coupling matrix element and the ET rate were also examined using the MP2 method. The results show that ET can occur over a considerable range of encounter distances. For the $H_3N\cdots NH_3^+$ coupling system, the ET occurs chiefly over a range of contact distances where $1.9\,\text{Å} < R_{N\text{—}N} < 4.0\,\text{Å}$. However, for the methyl-substituted coupling systems, the most effective contact distance range shifts to larger values. Namely, for the $CH_3H_2N\cdots NH_2CH_3^+$ coupling system, ET occurs chiefly over a range of contact distance where $2.5\,\text{Å} < R_{N\text{—}N} < 5.0\,\text{Å}$, whereas for the $(CH_3)_2HN\cdots NH(CH_3)_2^+$ and $N(CH_3)_3\cdots N(CH_3)_3^+$ coupling systems, the most favorable contact distance ranges to ET are $2.1\,\text{Å} < R_{N\text{—}N} < 5.0\,\text{Å}$ and $3.2\,\text{Å} < R_{N\text{—}N} < 6.0\,\text{Å}$, respectively.

For the $H_3N\cdots NH_3^+$, $CH_3H_2N\cdots NH_2CH_3^+$, $(CH_3)_2HN\cdots NH(CH_3)_2^+$ and $(CH_3)_3N\cdots N(CH_3)_3^+$ coupling systems, the optimum contact distances for ET with the largest rate are about 2.40, 3.0, 2.7, and 3.7 Å, respectively, and the corresponding maximum ET rates are $2.53\times10^5\,s^{-1}(H_3N\cdots NH_3^+)$, $1.16\times10^3\,s^{-1}$ $(CH_3H_2N\cdots NH_2CH_3^+)$, $7.55\times10^{-3}\,s^{-1}$ $[(CH_3)_2HN\cdots NH(CH_3)_2^+]$ and $2.25\times10^{-4}\,s^{-1}$ $[(CH_3)_3N\cdots N(CH_3)_3^+]$, respectively, in the order $H_3N\cdots NH_3^+ > CH_3H_2N\cdots NH_2CH_3^+ > (CH_3)_2HN\cdots NH(CH_3)_2^+ > (CH_3)_3N\cdots N(CH_3)_3^+$. It should be noted that for the $(CH_3)_{3-n}H_n$ $N\cdots NH_n(CH_3)_{3-n}^+$ coupling system, an increase in the number of methyl or other alkyl groups may disfavor the ET. However, whether an increase in the number of electron-donating groups may favors the ET or not needs further investigation. Obviously this work has provided some helpful information for deeper studies concerning the ET reactivity occurring between N-centered active sites in amino residues, peptides, proteins, DNA and other biological molecules containing active amino groups. Hence it will be very interesting to explore the ET reactivity between N-containing active centers and its substituent effect.

Acknowledgments

This work was supported by the National Natural Science Foundation of China (20273040) and the Natural Science Foundation of Shandong Province (Key Project). The support from SRFDP is also acknowledged.

REFERENCES

1. Bisling P, Rühl E, Brustchy B, Baumgürtel H. *J. Phys. Chem.* 1987; **91**: 4310–4317.
2. Brutschy B, Bisking P, Ruhl E, Baumartel H. *Z. Phys. D* 1987; **5**: 217–231.
3. Brutschy B. *J. Phys. Chem.* 1990; **94**: 8637–8647.
4. Marten B, Kim K, Cortis C, Friesner RA. *J. Phys. Chem.* 1996; **100**: 11775–11788.
5. Tzeng WB, Nararyanan K, Chang GC. *J. Phys. Chem.* 1996; **100**: 15340–15345.
6. Newton MD. *Int. J. Quantum Chem. Quantum Chem. Symp.* 1980; **14**: 363–391.
7. Cannon RD. *Electron Transfer Reactions*. Butterworth: London, 1980.
8. Sider P, Macus RA. *J. Am. Chem. Soc.* 1981; **103**: 748–752.
9. Tunuli MS, Khan SUM. *J. Phys. Chem.* 1987; **91**: 3474–3478.
10. Delahay P. *Chem. Phys. Lett.* 1982; **87**: 607–611.
11. Delahay P, Ziedzic AD. *J. Chem. Phys.* 1984; **80**: 5793–5798.
12. Bally T, Sastry GN. *J. Phys. Chem. A* 1997; **101**: 7923–7926.
13. Bu Y-X, Deng C-H. *J. Phys. Chem.* 1996; **100**: 18093–18100.
14. Bu Y-X, Song X-Y, Liu CB. *J. Phys. Chem. A* 1999; **103**: 4485–4493.
15. Bu Y-X, Cao ZH, Song X-Y. *Int. J. Quantum Chem.* 1996; **57**: 95–104.
16. Bu Y-X, Ding Y-J, Deng C-H. *J. Mol. Struct. (THEOCHEM)* 1997; **417**: 69–80.
17. Bu Y-X, Deng C-H. *J. Phys. Chem. A* 1997; **101**: 1198–1205.
18. Frisch MJ, Trucks GW, Schlegel HB, Gill PMW, Johnson BG, Robb MA, Cheeseman JR, Keith T, Petersson GA, Montgomery JA, Raghavachari K, Al-Laham MA, Zakrzewski VG, Ortiz JV, Foresman JB, Peng CY, Ayala PY, Chen W, Wong MW, Andres JL, Replogle ES, Gomperts R, Martin RL, Fox DJ, Binkley JS, Defrees DJ, Baker J, Stewart JP, Head-Gordon M, Gonzalez C, Pople JA. *Gaussian 94, Revision B.2*. Gaussian: Pittsburgh, PA, 1995.
19. Lee C, Yang W, Parr RG. *Phys. Rev. B* 1988; **37**: 785–789.
20. Stephens PJ, Devlin FJ, Ashvar CS, Chabalowki CF, Frisch MJ. *Faraday Discuss. Chem. Soc.* 1994; **99**: 103–119.
21. Perdew JP. *Phys. Rev. B* 1986; **33**: 8822–8824.
22. Perdew JP. *Phys. Rev. B* 1986; **34**: 7406.
23. Perdew JP, Wang Y. *Phys. Rev. B* 1992; **45**: 13244–13249.
24. Kari RE, Csizimadia IG. *J. Chem. Phys.* 1972; **56**: 4337–4344.
25. Hinchcliffe A. *J. Mol. Struct*. 1975; **27**: 329–334.
26. Xie Y-M, Schaefer HF III, Fu X-Y, Liu R-Z. *J. Chem. Phys.* 1999; **111**: 2532–2541.
27. Hrouda V, Roeselova M, Bally T. *J. Phys. Chem. A* 1997; **101**: 3925–3935.
28. Sun Q, Bu Y-X, Qin M. *J. Phys. Chem. A* 2003; **107**: 1584–1596.
29. Reed AE, Curtiss LA, Weinhold FA. *Chem. Rev.* 1988; **88**: 899–926.
30. Marcus RA. *Annu. Rev. Phys. Chem.* 1964; **15**: 155–196.